bioRxiv preprint doi: https://doi.org/10.1101/348532; this version posted June 16, 2018. The copyright holder for this preprint (which was not certified by peer review) is the author/funder. All rights reserved. No reuse allowed without permission.

WDR5 regulates epithelial-to-mesenchymal transition in breast cancer cells *via* TGFβ

Punzi Simona[1], Balestrieri Chiara[1,10], D'Alesio Carolina[1,11], Bossi Daniela[1,12], Dellino Gaetano Ivan[1,2], Gatti Elena[1], Pruneri Giancarlo[3,4,13], Criscitiello Carmen[5], Carugo Alessandro[6], Curigliano Giuseppe[5,7], Natoli Gioacchino[1,8,10], Pelicci Pier Giuseppe[1,9], Lanfrancone Luisa[1 *].

Affiliations

[1]Department of Experimental Oncology, European Institute of Oncology, Milan, Italy

[2]Department of Oncology and Hemato-Oncology, University of Milan, Milan, Italy

[3]School of Medicine, University of Milan, 20122 Milan, Italy

[4]Biobank for Translational Medicine Unit, Department of Pathology, European Institute of Oncology, Milan 20141, Italy

[5]Division of Early Drug Development for Innovative Therapy, University of Milano, European Institute of Oncology, Milan, Italy

[6]Institute for Applied Cancer Science, UT MD Anderson Cancer Center, Houston, TX 77030, USA

[7]Department of Oncology and Hemato-Oncology, University of Milano, European Institute of Oncology, Milan, Italy

[8]Humanitas Clinical and Research Institute, Rozzano, Milan, Italy.

[9]Department of Oncology, University of Milan, Milan, Italy

Current address:

[10]Department of Biomedical Sciences, School of Medicine, Humanitas University, Pieve Emanuele, Milan, Italy.

bioRxiv preprint doi: https://doi.org/10.1101/348532; this version posted June 16, 2018. The copyright holder for this preprint (which was not certified by peer review) is the author/funder. All rights reserved. No reuse allowed without permission.

[11]Department of Internal Medicine and Medical Specialities (Di.M.I), University of Genova, Genova, Italy,

[12]Institute of Oncology Research (IOR), Bellinzona, Switzerland.

[13]Istituto Nazionale dei Tumori – Fondazione IRCCS, Milan, Italy

*: Corresponding author email: luisa.lanfrancone@ieo.it

bioRxiv preprint doi: https://doi.org/10.1101/348532; this version posted June 16, 2018. The copyright holder for this preprint (which was not certified by peer review) is the author/funder. All rights reserved. No reuse allowed without permission.

Abstract

Even if the mortality rate in breast cancer (BC) has recently decreased, development of metastases and drug resistance are still challenges to successful systemic treatment. The epithelial-to-mesenchymal transition (EMT), as well as epigenetic dynamic modifications, plays a pivotal role in invasion, metastasis, and drug resistance. Here, we report that WDR5, the core subunit of histone H3 K4 methyltransferase complexes, is crucial in coordinating EMT and regulating epigenetic changes that drive metastasis. We show that silencing of WDR5 in BC up-regulates an epithelial signature in triple negative and luminal B like patients by transcriptional repression of mesenchymal genes and reduction of the metastatic properties of these cells. Moreover, we demonstrate that this regulation is mediated by inhibition of the TGFβ signaling both at the transcriptional and post-translational level, suggesting an active role of WDR5 in guiding tumor plasticity upon oncogenic insults, regardless of the pathological BC subtypes.

We therefore suggest that WDR5 inhibition could be a successful pharmacologic approach to inhibit EMT and sensitize breast cancer cells to chemotherapy.

Running title

WDR5 regulates EMT via TGFβ

Key words

Breast cancer/ EMT/ metastasis/ TGFβ/ WDR5

bioRxiv preprint doi: https://doi.org/10.1101/348532; this version posted June 16, 2018. The copyright holder for this preprint (which was not certified by peer review) is the author/funder. All rights reserved. No reuse allowed without permission.

Introduction

Despite recent advances in BC treatment, women frequently develop resistance to many therapies and die of metastasis (Ginsburg, Bray et al., 2017). Epithelial-to-mesenchymal transition (EMT) is a well-defined developmental program frequently adopted by tumor cells during the metastatic process to gain migratory ability and reach distant organs, losing epithelial cell adhesion and cell-cell contacts, while undergoing cell shape remodeling and cytoskeleton rearrangement (Christiansen & Rajasekaran, 2006, Nieto, 2013). Concurrently, the expression of epithelial markers is inhibited, in favor of an increase in the expression of the mesenchymal genes (Thiery & Sleeman, 2006). The epithelial and mesenchymal states represent two opposite cellular phenotypes that cells reach going through several intermediary phases (Grande, Sanchez-Laorden et al., 2015, Jordan, Johnson et al., 2011, Yu, Bardia et al., 2013).

During EMT, changes in gene expression are crucial for the process to occur. Availability of appropriate transcription factors and degree of openness or closeness of the chromatin play a central role in determining changes in gene expression (Bedi, Mishra et al., 2014). Indeed, the EMT transcriptional program is tightly controlled by both DNA methylation (Cedar & Bergman, 2009) and post-translational histone regulation (Campos & Reinberg, 2009). Even if the epigenetic contribution to the process is not fully understood, several histone modifications are implicated in either inducing or repressing specific sets of EMT genes (Lee & Kong, 2016). The core subunit of the COMPASS-like complex WD repeat-containing protein 5 (WDR5) recognizes the histone H3 amino-terminal tail, thus enabling its methylation on Lys4 (H3K4) (Ford & Dingwall, 2015). WDR5 has a pivotal role in tumor growth and proliferation (Carugo, Genovese et al., 2016, Chen, Xie et al., 2015, Mungamuri, Murk et al., 2013), differentiation (Ang, Tsai et al., 2011, Wang, Han et al., 2017) and metastasis (Lin, Wang et al., 2017, Malek, Gajula et al., 2017, Tan, Chen et al.,

bioRxiv preprint doi: https://doi.org/10.1101/348532; this version posted June 16, 2018. The copyright holder for this preprint (which was not certified by peer review) is the author/funder. All rights reserved. No reuse allowed without permission.

2017), showing deregulated expression in different cancers (Carugo et al., 2016, Chen et al., 2015, Cui, Li et al., 2018, Dai, Guo et al., 2015, Ge, Song et al., 2016, Wu, Diao et al., 2018b). Moreover, mesenchymal genes are marked with H3K4me3 by WDR5 in breast cancer upon hypoxia treatment (Wu, Tsai et al., 2011), and in colorectal (Tan et al., 2017), prostate (Malek et al., 2017), and lung [26] tumor cells. Despite its proven role in EMT, the causal role of WDR5 in cellular plasticity during EMT still remains elusive.

Transforming growth factor-β (TGFβ) is a multifunctional cytokine involved in a plethora of events regulating EMT in the context of metastasis. Both canonical and non-canonical TGFβ signaling are involved in the regulation of distinct processes as cytoskeleton organization, survival, cell migration and invasion (Micalizzi & Ford, 2009). It has been reported that TGFβ cooperates with other signaling pathways, as well as epigenetic regulators, in the induction of transcription factors, such as the SNAIL, ZEB and TWIST families, driving EMT (Cardenas, Zhao et al., 2016, Chen, Lorton et al., 2017).

Here, we demonstrate that WDR5 is directly involved in the epigenetic regulation of cellular plasticity in BC during EMT and that its inhibition reverts the mesenchymal phenotype mediated by the TGFβ1 response.

Results

WDR5 promotes growth of human breast cancer and is a potential therapeutic target

In our previous study, we performed a loss of function shRNA screening in the MCF10DCIS.com (hereafter MCF10DCIS) BC cell line to identify epigenetic targets driving tumorigenesis (D'Alesio, Punzi et al., 2016). Since WDR5 was strongly depleted both in the *in vivo* and *in vitro* screens and it ranked as one of the best candidate in sustaining BC

bioRxiv preprint doi: https://doi.org/10.1101/348532; this version posted June 16, 2018. The copyright holder for this preprint (which was not certified by peer review) is the author/funder. All rights reserved. No reuse allowed without permission.

growth (D'Alesio et al., 2016), we first validated its oncogenic role in MCF10DCIS cells. Cells were transduced with two pooled shRNAs to silence WDR5 and a corresponding control (shLuc) (Appendix Fig. S1A) and were either transplanted in NOD/SCID mice to assess *in vivo* tumor growth, or cultured to evaluate the *in vitro* proliferative ability. WDR5 silencing strongly reduced tumor growth *in vivo* (Fig. 1A), as well as proliferation *in vitro* (Fig. 1B), confirming that WDR5 is crucial in sustaining BC growth. Concordantly, we tested the efficacy of the WDR5 small molecule inhibitor, OICR-9429, already proven to be effective in leukemia, pancreatic and lung cancer cells (Carugo et al., 2016, Chen et al., 2017, Grebien, Vedadi et al., 2015). *In vitro* treatment of MFC10DCIS cells with OICR-9429 reduced clonogenicity (Fig. 1C) and proliferation (Fig. 1D) in a dose-dependent manner, similar to that observed by using shRNA.

In order to generate a reliable model to elucidate BC development and treatment opportunities, we created a bank of patient-derived xenografts (PDXs) obtained from liver and lung metastases of BC (MBC) patients who developed resistance to different lines of therapy (Appendix Table S1A). We demonstrated that PDXs recapitulate the phenotypic and molecular features of the tumors (Appendix Table S1B) and we used them as patient surrogates of the metastatic disease to investigate WDR5 expression. Since large evidence show the over-expression of WDR5 in diverse tumor types (Carugo et al., 2016, Chen et al., 2015, Cui et al., 2018, Ge et al., 2016, Wu et al., 2018b), we confirmed that WDR5 expression was significantly higher in MBC PDXs than in the normal mammary gland (Fig. 1E).

Six PDXs, representing triple negative (TN) and luminal B like (LB) BC subtypes, were used for the *in vivo* studies. Two TN (MBC2 and MBC7) and 4 LB (MBC3, MBC22, MBC18 and MBC26) PDXs were independently transduced with two shRNAs WDR5-specific in pool or a corresponding control (shLuc) (Appendix Fig. S1B). In parallel, we tested WDR5-

bioRxiv preprint doi: https://doi.org/10.1101/348532; this version posted June 16, 2018. The copyright holder for this preprint (which was not certified by peer review) is the author/funder. All rights reserved. No reuse allowed without permission.

silencing effects in highly aggressive TN (SUM149PTand MDAMB468) and LB (HCC1428 and ZR751) BC cell lines (Prat, Karginova et al., 2013) (Appendix Fig. S1C). The reduction of WDR5 expression significantly inhibited tumor growth in MBC PDXs (Fig. 1F) and in all tested cell lines (Appendix Fig. S1D). *In vitro* proliferation was also significantly impaired by shWDR5 (Appendix Fig. S1E), suggesting that WDR5 may be involved in tumorigenesis, independently of the BC subtypes.

WDR5 expression promotes breast cancer metastasization

Despite the fact that WDR5 has been reported to promote migration *in vitro* and metastasization *in vivo* in colon and prostate cancer cell lines (Malek et al., 2017, Tan et al., 2017), its role in BC is still unproven. We therefore compared the metastatic ability of shLuc and shWDR5 MDA-MB-231 cells by performing functional assays both *in vivo* and *in vitro*. Cells were first transduced with the Luciferase gene and then with either the WDR5 shRNA or the neutral control (SCR) and transplanted in the 4th mammary gland of NSG mice. Tumors were resected at the same volume in the control and WDR5-silenced groups (Appendix Fig. S2A) and mice were weekly tested for metastasis formation by bioluminescence assay. MDA-MB-231 metastasized to lung and axillary lymph nodes in SCR (Fig. 2A, upper panel) transplanted mice, while WDR5 silencing totally inhibited (3/5), or significantly reduced (2/5), the number and size of the metastatic foci (Fig. 2A, lower panel), as confirmed by the histological staining of the metastatic organs (Appendix Fig. S2B).

Modified Boyden chamber assay consistently demonstrated that WDR5 silencing led to a substantial reduction of the MDA-MB-231 cell migration (Fig. 2B), as well as in 6 MBC PDXs (Fig. 2C) and in MCF10DCIS (Appendix Fig. S2C) and the TN and LB cell lines (Appendix Fig. S2D) mentioned above. Concordantly, wound healing assay (Appendix Fig.

bioRxiv preprint doi: https://doi.org/10.1101/348532; this version posted June 16, 2018. The copyright holder for this preprint (which was not certified by peer review) is the author/funder. All rights reserved. No reuse allowed without permission.

S2E, S2F), performed in shWDR5 MDA-MB-231 cells, displayed a significant impairment of cell migration, as well. Overall these data suggest that WDR5 impacts on the ability of BC cells to migrate and metastasize to distant organs, and that its over-expression may be predictive of metastatic disease. To this aim, we analyzed WDR5 expression and Metastasis Free Survival (MFS) in a NKI data set of 295 patients, showing that higher WDR5 expression was associated with worse MFS (Fig. 2D), and that the prognostic role of WDR5 was independent of the hormonal and therapeutic status (Fig. 2E).

WDR5 silencing inhibits EMT in breast cancer

The ability of BC cells to metastasize has been correlated with the acquisition of an EMT phenotype (Chaffer, San Juan et al., 2016). Further, previous works suggested that WDR5 might regulate metastasis formation by inducing EMT in various cancers (Chen et al., 2017, Lin et al., 2017, Malek et al., 2017, Tan et al., 2017, Wu et al., 2011, Wu, Xiang et al., 2018a). We tested whether WDR5 silencing could reduce the migratory ability of BC cells by directly inhibiting EMT. As maintenance of the epithelial phenotype requires the coordinated expression of a set of genes directly implicated in cell adhesion and cytoskeletal polarization, we evaluated the transcriptional profile of control (shLuc) and shWDR5-silenced PDXs cells (2 TN and 3 LB) by RNA-seq. For each PDX we performed pairwise analysis to identify differentially expressed genes (DEGs) (Fig. 3A). In order to exclude individual specificities, possibly due to the intra- and inter-tumor heterogeneity of BC (Polyak, 2011), we considered a Golden Gene Set (GGS) of 161 down- and 92 up-regulated genes in common among at least 2 PDXs (Fig. 3B, Appendix Table S2). Gene Ontology (GO) analysis of GGS is shown in Figure 3C. Top ranking categories were related to cell polarization and adhesion, consistently reflecting changes in cell shape and cytoskeleton rearrangement that affect cell motility (Fig. 3C and Appendix Table S2). The

bioRxiv preprint doi: https://doi.org/10.1101/348532; this version posted June 16, 2018. The copyright holder for this preprint (which was not certified by peer review) is the author/funder. All rights reserved. No reuse allowed without permission.

inhibition of migratory cell ability may be in part explained by down-regulation of MAPRE1, a master regulator of microtubules (Rovini, Gauthier et al., 2013) and SDCBP, related to polarized distribution of F-actin (Das, Pradhan et al., 2018). Moreover, HSPA1B and PPME1 over-expression has been associated with poor survival of patients with ovarian, gastric and lung cancers (Jakobsson, Moen et al., 2015, Li, Han et al., 2014), suggesting that their down-modulation may reduce tumor progression. Concordantly, actin cytoskeleton rearrangements were detected in shLuc and shWDR5 MCF10DCIS cells. Immunofluorescence analysis revealed that filamentous actin (F-actin) was assembled into actin stress fibers in control cells, while in shWDR5 cells F-actin predominantly organized in cortical bundles tightly associated with cell-cell adhesions (Fig. 3D), reminiscent of an epithelial-like phenotype. We also investigated the adhesion properties of WDR5-silenced MCF10DCIS cells on a panel of extracellular matrices (collagen, laminin, fibronectin, matrigel), showing that cell adhesion is increased in shWDR5 cells both in term of cell number (Fig.3E and Appendix Fig. S3A) and cell spreading (Fig.3E and Appendix Fig. S3B), thus suggesting a tighter cell anchoring to the matrix.

We further characterized the expression of epithelial and mesenchymal markers in MBC PDXs in response to WDR5 silencing. WDR5 knockdown increased protein levels of E-cadherin (CDH1), a prominent biomarker of the epithelial state, while reduced the mesenchymal marker Vimentin (VIM) (Fig. 3F), suggesting that WDR5 may have a direct role in phenotype reversion. Moreover, the majority of genes acting as mesenchymal inducers or epithelial repressors, i.e. CDH2, TWIST1, SNAI1, SNAI2 and ZEB1, were transcriptionally down-modulated upon WDR5 silencing (Appendix Fig. S3C). Since, the transition from a mesenchymal to an epithelial state with drug treatment can be used to enhance lethality and eradicate epithelial cells, as well as a strategy to sensitize cells to chemotherapy (Meidhof, Brabletz et al., 2015), we used MCF10DCIS and MDA-MB-231 to

bioRxiv preprint doi: https://doi.org/10.1101/348532; this version posted June 16, 2018. The copyright holder for this preprint (which was not certified by peer review) is the author/funder. All rights reserved. No reuse allowed without permission.

test the effect of WDR5 inhibition on lethality and sensitization to paclitaxel (PTX). PTX administration, upon WDR5 silencing, significantly reduced MCF10DCIS cells viability after 72h of exposure with respect to WDR5-untreated cells (Appendix Fig. S3D). Interestingly, MDA-MB-231, that showed higher resistance to PTX, displayed significantly enhanced cell death also at low PTX doses upon WDR5 silencing (Appendix Fig. S3E).

Conversely, over-expression of WDR5 caused changes in cell morphology, leading to an elongated spindle shape of the cells (Appendix Fig. S4A), accompanied by the induction of mesenchymal gene expression (Appendix Fig. S4B), and increased tumorigenicity of MCF10DCIS cells *in vivo* (Appendix Fig. S4C). Overall, these observations suggest that WDR5 regulates the EMT program at transcriptional level in breast cancer cells and that its silencing can inhibit the mesenchymal phenotype.

WDR5 mediates epigenetic regulation of EMT

The EMT program is governed by a series of complex epigenetic interactions of transcription factors with protein complexes, whose mechanisms of action in driving plasticity during transition is still debated (Skrypek, Goossens et al., 2017). WDR5, as the core component of histone H3K4 methyltransferase complexes, is responsible of the methylation pattern of many EMT genes (Chen et al., 2017, Wu et al., 2011). We first analyzed WDR5 occupancy at the promoter regions of genes in MCF10DCIS cells by chromatin immunoprecipitation (ChIP) and sequencing. We found that around 80% (4413/5794) of the peaks were located proximal to the Transcription Start Sites (TSS) (± 3000 bp from TSS), confirming that WDR5 regulates its targets mainly at the promoter level (Fig. EV 1A). KMT2A/MLL1 and ERBB2, already known interactors of WDR5 (Ford & Dingwall, 2015, Mungamuri et al., 2013), are among these genes, thus validating our analysis. We also showed that TGFβ1, SMAD2 and SMAD3 and some members of the

bioRxiv preprint doi: https://doi.org/10.1101/348532; this version posted June 16, 2018. The copyright holder for this preprint (which was not certified by peer review) is the author/funder. All rights reserved. No reuse allowed without permission.

PI3K complex displayed a peak of WDR5 on their promoters, suggesting that WDR5 may be involved in multiple signaling regulation (Table EV 1). We performed additional RNA-seq analysis in shLuc and shWDR5 MCF10DCIS cells, and we detected 1'315 down- and 919 up-regulated DEGs. Diverse epithelial identity genes, keratins, genes regulating tight junctions and focal adhesions, as well as cell-cell adhesion molecules were found up-regulated (Fig. EV 1B). On the contrary, genes commonly involved in promoting mesenchymal phenotype and metastasis (i.e. TGFβ1, FOXQ1, ERBB3, S100A14, KIF4, CCR1, HAS2, PAK1 and TIAM1) were down-regulated (Fig. EV 1B), thus suggesting that WDR5 knockdown may sustain an epithelial phenotype. We therefore assessed H3K4me3 intensity at the promoter level of the expressed genes (± 1'500 bp from TSS) (Table EV 3) in MCF10DCIS cells, and we observed a global reduction of intensity in shWDR5 with respect to shLuc (*P*= 4.5E-9) (Fig. 4A). Remarkably, a statistical significant reduction in H3K4me3 intensity was observed at the promoter of the down-regulated (*P* = 1.2E-15), but not of up-regulated genes (Fig. 4A), confirming that the main effects due to WDR5 knockdown were observed in the down-modulated genes and that H3K4me3 signals, which associate with active and poised TSS, correlated with WDR5-dependent gene expression. We also determine level of H3K4me3 intensity at WDR5 peaks in the DEGs in MCF10DCIS cells. Among 907 hypo-methylated regions associated to gene promoters, 260 were found to show both differential expression and H3K4 trimethylation level (238 showed the same direction of alteration). Importantly, we detected 62 genes where WDR5 peaks are close to the TSS of the regulated genes (Fig. EV 1C). Among the top interesting ones we listed TGFβ1 (Fig. 4B), suggesting that WDR5 is essential for H3K4 methylation on TGFβ1 promoter and may be prominent for its activation. On the other side, among 698 hyper-methylated regions, 58 were also differentially expressed and 51 showed concordance in H3K4me3 increase. Only 5 out of 58 regions were directly bound by WDR5 (Fig. EV 1C).

bioRxiv preprint doi: https://doi.org/10.1101/348532; this version posted June 16, 2018. The copyright holder for this preprint (which was not certified by peer review) is the author/funder. All rights reserved. No reuse allowed without permission.

Interestingly, TGFβ signaling scored as one of the most significantly enriched biological functions in MBC PDXs (Appendix Table S2). The modulation of TGFβ-dependent pathways includes down-regulation of many oncogenes (Fig. 4C): (i) TGFβR2, as TGFβ type II receptor sustains metastasis of high-grade BC tumors (Tang, Vu et al., 2003); (ii) FURIN, a proprotein convertase that promotes the malignant phenotype of cancer cells (Jaaks & Bernasconi, 2017) and stimulate BC invasion (Li, Chu et al., 2018); (iii) GCNT2, that modulates EMT by modification of E-cadherin glycosylation (Zhang, Meng et al., 2011); (iv) PARD6, crucial for cell polarization (Mu, Zang et al., 2015) and (v) LTBP2, the Latent TGFβ-Binding protein, whose knock down inhibits tumorigenesis in thyroid carcinomas (Wan, Peng et al., 2017). Conversely, the tumor suppressor TGFβR3 was up-regulated in WDR5 silenced cells (Fig. 4C and Appendix Table S2), consistent with its role in suppressing metastasis formation in clear-cell renal cell carcinoma (Nishida, Miyazono et al., 2018). Finally, Ingenuity Pathway Analysis (IPA) confirmed that TGFβ1 resulted the top-ranking among genes or complexes that regulate EMT in breast cancer (HDAC3, ERBB2, HIF1A, SMAD7)(Ingthorsson, Andersen et al., 2016, Papageorgis, Lambert et al., 2010, Wu et al., 2011), as well as to be involved in tumor progression and metastatic dissemination (i.e. PI3K, E2F4, VEGFA and STAT3) (Beshiri, Holmes et al., 2012, Das et al., 2018, Jang, Kim et al., 2017, Tan et al., 2017). When transcriptomic profiles of the GGS of the PDXs and of the MCF10DCIS cells have been intersected, 99 down-regulated and 40 up-regulated genes were found in common (Fig. 4E). In details, we found that 6 out of 17 genes included in the TGFβ1-pathway have a role in sustaining cell migration in a number of cancer cells and were concordantly down-modulated in the majority of the MBC PDXs (Fig. 4F), as well as in MCF10DCIS (Fig. EV 1D). Interestingly, CEMIP (Cell Migration Inducing Hyaluronan Binding protein) expression regulates invasion and

bioRxiv preprint doi: https://doi.org/10.1101/348532; this version posted June 16, 2018. The copyright holder for this preprint (which was not certified by peer review) is the author/funder. All rights reserved. No reuse allowed without permission.

metastasis in colon cancer (Evensen, Li et al., 2015), HSPA1B (Heat Shock 70kDa Protein 1B) in ovarian cancer (Jakobsson et al., 2015), AIF1L (Allograft Inflammatory Factor 1 Like) determines cytoskeleton rearrangement (Lu, Ye et al., 2017), and PNP (purine nucleoside phosphorylase) affects prostate cell migration (Kojima, Chiyomaru et al., 2012), while the up-regulation of ECE1 (Endothelin Converting Enzyme 1) (Smollich, Gotte et al., 2007), GBP1 (Guanylate Binding Protein 1) (Pedersen, Hood et al., 2017), HMGCR (3-hydroxy-3-methylglutaryl-CoA reductase) (Singh, Yadav et al., 2015), PARD6A (par-6 family cell polarity regulator alpha) (Viloria-Petit, David et al., 2009) is linked to poor outcome and increased metastatic potential in BC.

WDR5 mediates the EMT response to TGFβ1

TGFβ1 is a pleiotropic cytokine that exerts several different functions in the cell, whose dysregulation mainly impacts on cancer progression and regulation of immune surveillance (David & Massague, 2018). Since our finding supported that WDR5 is required for EMT, as well as for TGFβ1 signaling during BC progression, we treated shLuc and shWDR5 MCF10DCIS cells with recombinant human TGFβ1. Then, we tested the relative expression of the mesenchymal genes known to be induced by TGFβ1, namely CDH2, TWIST1, SNAI1, SNAI2, ZEB1 (Micalizzi & Ford, 2009), also showed to be regulated in our PDXs. TGFβ1 dramatically increased the expression of these genes without altering WDR5 levels (Appendix Fig. S5A), while the WDR5 silencing strongly reduced TGFβ1-dependent transcription of these targets (Figure 5A). As shown in Figure 5B and Appendix Fig. S5B, cell migration was stimulated by TGFβ1 and restored to control levels in presence of WDR5 silencing, thus confirming that TGFβ1-induced migration and EMT is WDR5 dependent. Since it has been reported that TGFβ1 promotes EMT by a combination of canonical

bioRxiv preprint doi: https://doi.org/10.1101/348532; this version posted June 16, 2018. The copyright holder for this preprint (which was not certified by peer review) is the author/funder. All rights reserved. No reuse allowed without permission.

SMAD-dependent and non-canonical SMAD-independent transcriptional events (through the ERK1/2 pathway) (Felipe Lima, Nofech-Mozes et al., 2016), we wanted to confirm whether the TGFβ1 downstream mediators SMAD2/3 and ERK1/2 were also prominent for WDR5 regulation of TGFβ1 signaling. In our system, SMAD2, but not SMAD3, was phosphorylated by TGFβ1, while silencing of WDR5 reduced the phosphorylation of both substrates (Fig. 5C). Also, phosphorylation of ERK1/2, induced by TGFβ1, was inhibited by shWDR5 (Fig. 5D), thus confirming that various integrated signaling pathways are required for the regulation of WDR5 on TGFβ1.

Discussion

A extensive body of literature supports the essential role of WDR5 in targeting histones to epigenetically regulate cancer progression (Carugo et al., 2016, Chen et al., 2017, Ge et al., 2016, Mungamuri et al., 2013). TGFβ signaling and EMT are strictly interconnected pathways mediated by many key factors including epigenetic and transcriptional regulation (Dumont, Wilson et al., 2008). In this study we report that WDR5 is an essential gene in breast cancer development and progression that works as a crucial intermediate in coupling TGFβ pathway and EMT.

It has been previously shown that WDR5 expression is frequently deregulated in leukemia, colon, pancreatic and prostate cancer (Carugo et al., 2016, Chen et al., 2015, Cui et al., 2018, Ge et al., 2016, Tan et al., 2017). Here, we directly link WDR5 expression to breast cancer progression and metastasis by using a panel of cell lines and PDX models of metastatic breast cancer resistant to different lines of therapy. For these patients offering new therapeutic strategies is mandatory. For *in vitro* and *in vivo* studies, we made use of the highly plastic MCF10DCIS breast cancer cell line, known to be able to recapitulate all

bioRxiv preprint doi: https://doi.org/10.1101/348532; this version posted June 16, 2018. The copyright holder for this preprint (which was not certified by peer review) is the author/funder. All rights reserved. No reuse allowed without permission.

the stages of breast cancer progression, from *in situ* growth to metastasis formation (Barnabas & Cohen, 2013, D'Alesio et al., 2016). MCF10DCIS cells appear to be the most attractive model to study the molecular mechanisms responsible of the epigenetic regulation in the transition from the epithelial to the mesenchymal state and *viceversa*.

WDR5 knockdown was able to reduce tumor growth in LB and TN breast cancers, concordantly with the role of WDR5 in regulating tumorigenesis (Carugo et al., 2016, Chen et al., 2015, Mungamuri et al., 2013). We offered direct evidences of the involvement of WDR5 in breast cancer progression by performing a meta-analysis on metastasis free survival in breast cancer patients, as well as by using *in vivo* MDA-MB-231 cells and *in vitro* migratory PDXs.

By employing gene expression profiling of differentially expressed genes in PDXs and breast cancer cell line models, we found that WDR5 transcriptionally regulates an epithelial signature and induce cell adaptation to signaling events. Among these, TGFβ regulation is affected by down-modulation of TGFβ receptors and downstream targets genes that were reported to control cell migration in tumors (Evensen et al., 2015, Jaaks & Bernasconi, 2017, Kojima et al., 2012, Lu et al., 2017, Mu et al., 2015, Pedersen et al., 2017, Singh et al., 2015, Smollich et al., 2007, Tang et al., 2003, Viloria-Petit et al., 2009, Wan et al., 2017, Zhang et al., 2011) (Fig. 6A). By examining the genome wide WDR5 occupancy, we show that WDR5 directly binds to a subset of gene promoters, among which we highlighted TGFβ1, suggesting that WDR5 activates TGFβ oncogenic pathways known to be involved in tumorigenesis and metastasis (Felipe Lima et al., 2016). Indeed, transcriptional regulation of WDR5 targets occurs through recruitment of KMT2A in the COMPASS-like complex, and subsequent methylation of H3K4 (Alicea-Velazquez, Shinsky et al., 2016). Our data suggest that a similar mechanism is in place also in breast cancer, as WDR5-dependent, down-regulated genes are hypomethylated in WDR5 silenced cells. TGFβ1

bioRxiv preprint doi: https://doi.org/10.1101/348532; this version posted June 16, 2018. The copyright holder for this preprint (which was not certified by peer review) is the author/funder. All rights reserved. No reuse allowed without permission.

signaling has been widely associated with the EMT phenotype (David & Massague, 2018). Mimicking microenvironmental sources, TGFβ1 administration maintains TGFβ signaling overactive and sustains invasive properties of BC cells by altering many EMT transcriptional drivers, including TWIST1, SNAI1, SNAI2 and ZEB1. It is well known that these transcription factors may recruits chromatin modifiers (HDAC1, HDAC2, LSD1, PRC2 complex) by activating dynamic chromatin control loop of their targets (Herranz, Pasini et al., 2008, Lin, Ponn et al., 2010, Peinado, Ballestar et al., 2004) and contributing to the plasticity during transition. EMT induced by exogenous TGFβ was significantly impaired by WDR5 silencing, by reducing transcription of many EMT genes and bringing the cells to an intermediated metastable state. This effect also reflects the flexibility of these cells to undergo EMT, or revert the mesenchymal phenotype, leading to metastasis (Bedi et al., 2014) (Fig. 6B). Finally, WDR5 is instrumental in allowing TGFβ canonical (SMADs) and non-canonical (ERK1/2) -dependent activation since the impact on phosphorylation strongly implies a direct involvement of WDR5 in the post-translational modulation of the TGFβ machinery.

Overall, we suggest a key role of WDR5 in cell program by driving tumor plasticity upon oncogenic insults. Reversion of the EMT program by inhibition of WDR5 represents a captivating therapeutic option, in particular for drug-resistant patients. In fact, we have shown that WDR5 inhibition can sensitize breast cancer cells to paclitaxel even at low doses, suggesting a promising way of counteracting the onset of resistance to second line therapies. These observations are encouraging for further clinical investigation and suggest that WDR5 inhibition could be a novel therapeutic approach to prevent tumor metastasis in breast cancer.

bioRxiv preprint doi: https://doi.org/10.1101/348532; this version posted June 16, 2018. The copyright holder for this preprint (which was not certified by peer review) is the author/funder. All rights reserved. No reuse allowed without permission.

Methods

PDX tissue bank generation. Patients enrolled in the study were selected on the basis of highly aggressive metastatic disease diagnoses (Luminal B and Triple Negative subtypes) and resistance to different lines of therapy. Biopsies from liver and lung were transplanted in Matrigel (Corning #356231) orthotopically in the 4th mammary gland of female NSG mice. Tumors were monitored weekly and serially passaged in NSG after tissue digestion (see "PDX culture"). Tumors were characterized by IHC on the basis of the prognostic clinical markers, i.e. Estrogen, Progesterone, HER2 and Ki67, by pathologists and compared to patient tumors. Positive staining is expressed as percentage.

Animals. Non-obese diabetic/severe combined immunodeficiency (NOD/SCID) mice were purchased from Harlan Laboratories. NOD.Cg-Prkdc^{scid} Il2rg^{tm1Wjl}/SzJ (NSG) mice were purchased from Charles River. Only female mice 6-12 weeks old (15-20 gr weight) were used for experimental procedures.

Ethic statements. Investigations have been conducted in accordance with the ethical standards and according to National and International guidelines. *In vivo* studies were performed after approval from our fully authorized animal facility, notification of the experiments to the Ministry of Health (as required by the Italian Law) (IACUCs N° 757/2015, 1246/2015 and 327/2016) and in accordance to EU directive 2010/63. Human tissue biopsies were collected from patients whose informed consent was obtained in writing according to the policies of the Ethics Committee of the European Institute of Oncology and regulations of Italian Ministry of Health. The studies were conducted in full compliance with the Declaration of Helsinki.

bioRxiv preprint doi: https://doi.org/10.1101/348532; this version posted June 16, 2018. The copyright holder for this preprint (which was not certified by peer review) is the author/funder. All rights reserved. No reuse allowed without permission.

PDX culture. PDX tumors were dissociated by enzymatic and mechanical digestion (Miltenyi Biotec) and cells were plated to obtain short-term cultures. PDX cells were maintained in DMEM/F12 (1:1, Lonza/ Gibco) supplemented with 10% Fetal Bovine Serum (FBS) (HyClone, GE Healthcare Life Science), 10mM HEPES (Sigma), 5 µg/mL insulin (Roche), 0.5 µg/mL hydrocortisone (Sigma), 10 ng/mL epidermal growth factor (EGF, Tebu-Bio), 50 ng/mL Cholera Toxin (Sigma).

Cell lines. Experiments were performed in: MCF10DCIS.com (from Wayne State University, 5057 Woodward Avenue, Detroit - Michigan), SUM149PT (from Asterand), HCC1428 (from IFOM), MDA-MB-468 (from CLS), ZR751 (from ATCC) and MDA-MB-231 (from NIH Institute) cell lines were maintained in their respective media as recommended by suppliers. Cell line authentication was performed in house by Gene Print 10 System every six months (Promega). All cell lines were tested for mycoplasma and resulted negative.

***In vivo* study**. PDXs, MCF10DCIS.com, SUM149PT, HCC1428, MDAMB468 and ZR751 were infected with control shRNA (shLuc) and pooled shWDR5. 2.5^10^5 infected cells were orthotopically injected into the 4th mammary gland of 3 to 8 mice (MCF10DCIS.com were transplanted in NOD/SCID mice; PDXs cells, SUM149PT, HCC1428, MDAMB468 AND ZR751 in NSG mice). Tumor volume was calculated using this formula: V=l^2^L/2 (l length; L width). MDA-MB-231 cells were transfected with the luciferase plasmid (Addgene 17477) and selected by using Puromycin. Cells were then transfected to silence shLuc or shWDR5 and then 2^10^5 transplanted in the 4th mammary gland of 5 NSG mice *per* group. The mice were monitored for primary tumor growth. When a volume of about 0.5 cm^3 was reached, tumors were excised and mice monitored weekly for metastasis formation. Luciferase

bioRxiv preprint doi: https://doi.org/10.1101/348532; this version posted June 16, 2018. The copyright holder for this preprint (which was not certified by peer review) is the author/funder. All rights reserved. No reuse allowed without permission.

expression was assessed by bioluminescence imaging (IVIS Lumina Imaging System - PerkinElmer) and mice were sacrificed one month after resection, when lungs and axillary lymph nodes resulted positive to luminescence. Organs were fixed in paraffin, sectioned and Hematoxylin and eosin (H&E) stained.

***In vitro* study.** Proliferation, migration on Boyden chamber and wound healing assays were performed as described in expanded view.

Immunofluorescence. MCF10DCIS.com cells were infected to silence shLuc or sWDR5 and after two days of infection 1^10^5 cells were plated on slides and allowed to attach overnight. Next day, cells were fixed with 4% paraformaldhehyde for 10 minutes, permeabilized with 0.01% Triton-X and blocked for 1h with 2% bovine serum albumine. The actin cytoskeleton was stained using FITC-labeled Phalloidin from Sigma (P5282) for 2 hours. Slides were then counterstained with 4',6-diamidino-2-phenylindole (DAPI) for nuclei labelling and mounted on glass slides with Mowiol. Images were collected by motorized Olympus fluorescence microscope at 40X magnification.

Adhesion assay. For adhesion assay, 2^10^4 shLuc and shWDR5 MCF10DCIS.com cells were plated onto different extracellular matrices (collagen - CL, laminin - LM, fibronectin - FN, matrigel – MG). After 1.5 hour, cells were fixed and stained with 0.5% Crystal Violet. Three images *per* well were acquired and cell number and area were quantified by using ImageJ software by manually delineating the edges of randomly selected cells (a total of 30 measurements *per* group) and recording the circularity value.

bioRxiv preprint doi: https://doi.org/10.1101/348532; this version posted June 16, 2018. The copyright holder for this preprint (which was not certified by peer review) is the author/funder. All rights reserved. No reuse allowed without permission.

Western blot. PDXs and MCF10DCIS.com cells were lysed in RIPA buffer and processed, as previously described (D'Alesio et al., 2016). Membranes were probed with antibodies reported in expanded. Images were cropped at specific protein band of interest to improve the clarity of data presentation.

Survival Analysis. Association between WDR5 expression and metastasis free survival (MFS) in 295 breast cancer patients was calculated using PROGgene V2 software on NKI data sets. MFS were represented by Kaplan-Meier functions and cohorts were divided at the median of gene expression. Statistic comparison between high and low expression groups was performed using log rank test. Differences were considered significant at $P < 0.05$.

RNA-sequencing. Total RNA was extracted from shLuc and shWDR5 MCF10DCIS.com cells or PDXs infected cells by using the Maxwell 16LEV simply RNA tissue kit. mRNA purification and NGS libraries were obtained following Illumina instruction (TruSeq RNA Sample Preparation). Bioinformatic analysis is fully described in Appendix Supplementary Methods.

ChIP-sequencing. ChIP lysates were generated from 10-15^10^6 cells as reported previously (Bossi, Cicalese et al., 2016). ChIP DNA was prepared for HiSeq 2000 Illumina sequencing. Samples were aligned to human genome and bioinformatic analysis is fully described in Appendix Supplementary Methods.

bioRxiv preprint doi: https://doi.org/10.1101/348532; this version posted June 16, 2018. The copyright holder for this preprint (which was not certified by peer review) is the author/funder. All rights reserved. No reuse allowed without permission.

Data Access

Data sets are available in the Gene Expression Omnibus (GEO) database under accession number GSE113289 .

Quantitative RT-PCR. Total RNA was extracted from PDXs and MCF10DCIS.com as above and reverse transcribed using OneScript Plus Reverse Transcriptase and cDNA Synthesis kit (abm). Quantitative RT-PCR analyses were done on Biorad CFX Real-Time PCR System with the fast-SYBR Green PCR kit as instructed by the manufacturer (Applied Biosystems). The transcription level of the RPLP0 housekeeper gene was used as normalizer. Complete primers sequences are reported in Appendix Table S3.

Drugs treatment. 1.5^10^6 cells were plated on 10cm plates. Recombinant human TGFβ1 (Peprotech) was added at a final concentration of 5ng/ml for 2 days. OICR-9429 was obtained from MD Anderson Cancer Center (Texas) and resuspended in DMSO. 1.5^10^5 MCF10DCIS.com were plated in six-well plates. Drug was added to complete medium at a final concentration of 1μM - 5μM - 10μM or 20μM for 3 days and cells were then effects on proliferation was assessed. 10^3 cells were plated for colony formation assay and drug was added for 6 days (medium and drug was refreshed on day 3). Cells were then stained with Crystal violet and quantified by ImageJ analysis.

Statistical analysis. Data are represented as mean ± SD of triplicate biological replicates (if not diversely indicated in the text) and have been statistically assessed by two-tailed Student's *t* test as indicate in figure legend. In figures, asterisks mean * $p<0.05$, ** $p<0.01$, *** $p<0.001$. $p<0.05$ and lower were considered significant. For RNA-seq and ChIP-seq analysis, statistical parameters are indicated in Appendix Supplementary methods.

bioRxiv preprint doi: https://doi.org/10.1101/348532; this version posted June 16, 2018. The copyright holder for this preprint (which was not certified by peer review) is the author/funder. All rights reserved. No reuse allowed without permission.

Acknowledgments

S. Punzi is recipient of a FUV fellowship. This work was supported by the European Research Council Advanced Grant 341131. We thank A. De Rose and R. Piccioni for technical support. We also thank A. Gobbi and M. Capillo for excellent support in animal work. We wish to thank all members of the Department of Experimental Oncology for discussion and reagents. We thank the Genomic Unit (IEO), the Mouse Facility (Cogentech), Istituto Italiano di Tecnologia (IIT) and the Cell Biology Unit (IEO).

Author contribution

S.P., L.L., conceived the study, designed the experiments and interpreted the data. C.B. performed computational analysis. C.D., D.B., A.C., G.I.D. and E.G. provided essential reagents and expertise. G.P., C.C. and G.C. managed patients. P.G.P, G.N. reviewed critically the work. L.L. supervised the work. S.P. and L.L. wrote the manuscript.

Competing Interests

The authors declare no competing interest

bioRxiv preprint doi: https://doi.org/10.1101/348532; this version posted June 16, 2018. The copyright holder for this preprint (which was not certified by peer review) is the author/funder. All rights reserved. No reuse allowed without permission.

References

Alicea-Velazquez NL, Shinsky SA, Loh DM, Lee JH, Skalnik DG, Cosgrove MS (2016) Targeted Disruption of the Interaction between WD-40 Repeat Protein 5 (WDR5) and Mixed Lineage Leukemia (MLL)/SET1 Family Proteins Specifically Inhibits MLL1 and SETd1A Methyltransferase Complexes. J Biol Chem 291: 22357-22372

Ang YS, Tsai SY, Lee DF, Monk J, Su J, Ratnakumar K, Ding J, Ge Y, Darr H, Chang B, Wang J, Rendl M, Bernstein E, Schaniel C, Lemischka IR (2011) Wdr5 mediates self-renewal and reprogramming via the embryonic stem cell core transcriptional network. Cell 145: 183-97

Barnabas N, Cohen D (2013) Phenotypic and Molecular Characterization of MCF10DCIS and SUM Breast Cancer Cell Lines. Int J Breast Cancer 2013: 872743

Bedi U, Mishra VK, Wasilewski D, Scheel C, Johnsen SA (2014) Epigenetic plasticity: a central regulator of epithelial-to-mesenchymal transition in cancer. Oncotarget 5: 2016-29

Beshiri ML, Holmes KB, Richter WF, Hess S, Islam AB, Yan Q, Plante L, Litovchick L, Gevry N, Lopez-Bigas N, Kaelin WG, Jr., Benevolenskaya EV (2012) Coordinated repression of cell cycle genes by KDM5A and E2F4 during differentiation. Proc Natl Acad Sci U S A 109: 18499-504

Bossi D, Cicalese A, Dellino GI, Luzi L, Riva L, D'Alesio C, Diaferia GR, Carugo A, Cavallaro E, Piccioni R, Barberis M, Mazzarol G, Testori A, Punzi S, Pallavicini I, Tosti G, Giaco L, Melloni G, Heffernan TP, Natoli G et al. (2016) In Vivo Genetic Screens of Patient-

bioRxiv preprint doi: https://doi.org/10.1101/348532; this version posted June 16, 2018. The copyright holder for this preprint (which was not certified by peer review) is the author/funder. All rights reserved. No reuse allowed without permission.

Derived Tumors Revealed Unexpected Frailty of the Transformed Phenotype. Cancer Discov 6: 650-63

Campos EI, Reinberg D (2009) Histones: annotating chromatin. Annu Rev Genet 43: 559-99

Cardenas H, Zhao J, Vieth E, Nephew KP, Matei D (2016) EZH2 inhibition promotes epithelial-to-mesenchymal transition in ovarian cancer cells. Oncotarget 7: 84453-84467

Carugo A, Genovese G, Seth S, Nezi L, Rose JL, Bossi D, Cicalese A, Shah PK, Viale A, Pettazzoni PF, Akdemir KC, Bristow CA, Robinson FS, Tepper J, Sanchez N, Gupta S, Estecio MR, Giuliani V, Dellino GI, Riva L et al. (2016) In Vivo Functional Platform Targeting Patient-Derived Xenografts Identifies WDR5-Myc Association as a Critical Determinant of Pancreatic Cancer. Cell Rep 16: 133-147

Cedar H, Bergman Y (2009) Linking DNA methylation and histone modification: patterns and paradigms. Nat Rev Genet 10: 295-304

Chaffer CL, San Juan BP, Lim E, Weinberg RA (2016) EMT, cell plasticity and metastasis. Cancer Metastasis Rev 35: 645-654

Chen H, Lorton B, Gupta V, Shechter D (2017) A TGFbeta-PRMT5-MEP50 axis regulates cancer cell invasion through histone H3 and H4 arginine methylation coupled transcriptional activation and repression. Oncogene 36: 373-386

bioRxiv preprint doi: https://doi.org/10.1101/348532; this version posted June 16, 2018. The copyright holder for this preprint (which was not certified by peer review) is the author/funder. All rights reserved. No reuse allowed without permission.

Chen X, Xie W, Gu P, Cai Q, Wang B, Xie Y, Dong W, He W, Zhong G, Lin T, Huang J (2015) Upregulated WDR5 promotes proliferation, self-renewal and chemoresistance in bladder cancer via mediating H3K4 trimethylation. Sci Rep 5: 8293

Christiansen JJ, Rajasekaran AK (2006) Reassessing epithelial to mesenchymal transition as a prerequisite for carcinoma invasion and metastasis. Cancer Res 66: 8319-26

Cui Z, Li H, Liang F, Mu C, Mu Y, Zhang X, Liu J (2018) Effect of high WDR5 expression on the hepatocellular carcinoma prognosis. Oncol Lett 15: 7864-7870

D'Alesio C, Punzi S, Cicalese A, Fornasari L, Furia L, Riva L, Carugo A, Curigliano G, Criscitiello C, Pruneri G, Pelicci PG, Faretta M, Bossi D, Lanfrancone L (2016) RNAi screens identify CHD4 as an essential gene in breast cancer growth. Oncotarget 7: 80901-80915

Dai X, Guo W, Zhan C, Liu X, Bai Z, Yang Y (2015) WDR5 Expression Is Prognostic of Breast Cancer Outcome. PLoS One 10: e0124964

Das SK, Pradhan AK, Bhoopathi P, Talukdar S, Shen XN, Sarkar D, Emdad L, Fisher PB (2018) The MDA-9/Syntenin/IGF1R/STAT3 Axis Directs Prostate Cancer Invasion. Cancer Res

David CJ, Massague J (2018) Contextual determinants of TGFbeta action in development, immunity and cancer. Nat Rev Mol Cell Biol

bioRxiv preprint doi: https://doi.org/10.1101/348532; this version posted June 16, 2018. The copyright holder for this preprint (which was not certified by peer review) is the author/funder. All rights reserved. No reuse allowed without permission.

Dumont N, Wilson MB, Crawford YG, Reynolds PA, Sigaroudinia M, Tlsty TD (2008) Sustained induction of epithelial to mesenchymal transition activates DNA methylation of genes silenced in basal-like breast cancers. Proc Natl Acad Sci U S A 105: 14867-72

Evensen NA, Li Y, Kuscu C, Liu J, Cathcart J, Banach A, Zhang Q, Li E, Joshi S, Yang J, Denoya PI, Pastorekova S, Zucker S, Shroyer KR, Cao J (2015) Hypoxia promotes colon cancer dissemination through up-regulation of cell migration-inducing protein (CEMIP). Oncotarget 6: 20723-39

Felipe Lima J, Nofech-Mozes S, Bayani J, Bartlett JM (2016) EMT in Breast Carcinoma-A Review. J Clin Med 5

Ford DJ, Dingwall AK (2015) The cancer COMPASS: navigating the functions of MLL complexes in cancer. Cancer Genet 208: 178-91

Ge Z, Song EJ, Kawasawa YI, Li J, Dovat S, Song C (2016) WDR5 high expression and its effect on tumorigenesis in leukemia. Oncotarget 7: 37740-37754

Ginsburg O, Bray F, Coleman MP, Vanderpuye V, Eniu A, Kotha SR, Sarker M, Huong TT, Allemani C, Dvaladze A, Gralow J, Yeates K, Taylor C, Oomman N, Krishnan S, Sullivan R, Kombe D, Blas MM, Parham G, Kassami N et al. (2017) The global burden of women's cancers: a grand challenge in global health. Lancet 389: 847-860

Grande MT, Sanchez-Laorden B, Lopez-Blau C, De Frutos CA, Boutet A, Arevalo M, Rowe RG, Weiss SJ, Lopez-Novoa JM, Nieto MA (2015) Snail1-induced partial epithelial-to-

bioRxiv preprint doi: https://doi.org/10.1101/348532; this version posted June 16, 2018. The copyright holder for this preprint (which was not certified by peer review) is the author/funder. All rights reserved. No reuse allowed without permission.

mesenchymal transition drives renal fibrosis in mice and can be targeted to reverse established disease. Nat Med 21: 989-97

Grebien F, Vedadi M, Getlik M, Giambruno R, Grover A, Avellino R, Skucha A, Vittori S, Kuznetsova E, Smil D, Barsyte-Lovejoy D, Li F, Poda G, Schapira M, Wu H, Dong A, Senisterra G, Stukalov A, Huber KVM, Schonegger A et al. (2015) Pharmacological targeting of the Wdr5-MLL interaction in C/EBPalpha N-terminal leukemia. Nat Chem Biol 11: 571-578

Herranz N, Pasini D, Diaz VM, Franci C, Gutierrez A, Dave N, Escriva M, Hernandez-Munoz I, Di Croce L, Helin K, Garcia de Herreros A, Peiro S (2008) Polycomb complex 2 is required for E-cadherin repression by the Snail1 transcription factor. Mol Cell Biol 28: 4772-81

Ingthorsson S, Andersen K, Hilmarsdottir B, Maelandsmo GM, Magnusson MK, Gudjonsson T (2016) HER2 induced EMT and tumorigenicity in breast epithelial progenitor cells is inhibited by coexpression of EGFR. Oncogene 35: 4244-55

Jaaks P, Bernasconi M (2017) The proprotein convertase furin in tumour progression. Int J Cancer 141: 654-663

Jakobsson ME, Moen A, Davidson B, Falnes PO (2015) Hsp70 (HSPA1) Lysine Methylation Status as a Potential Prognostic Factor in Metastatic High-Grade Serous Carcinoma. PLoS One 10: e0140168

bioRxiv preprint doi: https://doi.org/10.1101/348532; this version posted June 16, 2018. The copyright holder for this preprint (which was not certified by peer review) is the author/funder. All rights reserved. No reuse allowed without permission.

Jang K, Kim M, Gilbert CA, Simpkins F, Ince TA, Slingerland JM (2017) VEGFA activates an epigenetic pathway upregulating ovarian cancer-initiating cells. EMBO Mol Med 9: 304-318

Jordan NV, Johnson GL, Abell AN (2011) Tracking the intermediate stages of epithelial-mesenchymal transition in epithelial stem cells and cancer. Cell Cycle 10: 2865-73

Kojima S, Chiyomaru T, Kawakami K, Yoshino H, Enokida H, Nohata N, Fuse M, Ichikawa T, Naya Y, Nakagawa M, Seki N (2012) Tumour suppressors miR-1 and miR-133a target the oncogenic function of purine nucleoside phosphorylase (PNP) in prostate cancer. Br J Cancer 106: 405-13

Lee JY, Kong G (2016) Roles and epigenetic regulation of epithelial-mesenchymal transition and its transcription factors in cancer initiation and progression. Cell Mol Life Sci 73: 4643-4660

Li J, Han S, Qian Z, Su X, Fan S, Fu J, Liu Y, Yin X, Gao Z, Zhang J, Yu DH, Ji Q (2014) Genetic amplification of PPME1 in gastric and lung cancer and its potential as a novel therapeutic target. Cancer Biol Ther 15: 128-34

Li Y, Chu J, Li J, Feng W, Yang F, Wang Y, Zhang Y, Sun C, Yang M, Vasilatos SN, Huang Y, Fu Z, Yin Y (2018) Cancer/testis Antigen-Plac1 Promotes Invasion and Metastasis of Breast Cancer through Furin/NICD/PTEN Signaling Pathway. Molecular oncology

bioRxiv preprint doi: https://doi.org/10.1101/348532; this version posted June 16, 2018. The copyright holder for this preprint (which was not certified by peer review) is the author/funder. All rights reserved. No reuse allowed without permission.

Lin C, Wang Y, Wang Y, Zhang S, Yu L, Guo C, Xu H (2017) Transcriptional and posttranscriptional regulation of HOXA13 by lncRNA HOTTIP facilitates tumorigenesis and metastasis in esophageal squamous carcinoma cells. Oncogene 36: 5392-5406

Lin T, Ponn A, Hu X, Law BK, Lu J (2010) Requirement of the histone demethylase LSD1 in Snai1-mediated transcriptional repression during epithelial-mesenchymal transition. Oncogene 29: 4896-904

Lu Y, Ye Y, Bao W, Yang Q, Wang J, Liu Z, Shi S (2017) Genome-wide identification of genes essential for podocyte cytoskeletons based on single-cell RNA sequencing. Kidney Int 92: 1119-1129

Malek R, Gajula RP, Williams RD, Nghiem B, Simons BW, Nugent K, Wang H, Taparra K, Lemtiri-Chlieh G, Yoon AR, True L, An SS, DeWeese TL, Ross AE, Schaeffer EM, Pienta KJ, Hurley PJ, Morrissey C, Tran PT (2017) TWIST1-WDR5-Hottip Regulates Hoxa9 Chromatin to Facilitate Prostate Cancer Metastasis. Cancer Res 77: 3181-3193

Meidhof S, Brabletz S, Lehmann W, Preca BT, Mock K, Ruh M, Schuler J, Berthold M, Weber A, Burk U, Lubbert M, Puhr M, Culig Z, Wellner U, Keck T, Bronsert P, Kusters S, Hopt UT, Stemmler MP, Brabletz T (2015) ZEB1-associated drug resistance in cancer cells is reversed by the class I HDAC inhibitor mocetinostat. EMBO Mol Med 7: 831-47

Micalizzi DS, Ford HL (2009) Epithelial-mesenchymal transition in development and cancer. Future Oncol 5: 1129-43

bioRxiv preprint doi: https://doi.org/10.1101/348532; this version posted June 16, 2018. The copyright holder for this preprint (which was not certified by peer review) is the author/funder. All rights reserved. No reuse allowed without permission.

Mu Y, Zang G, Engstrom U, Busch C, Landstrom M (2015) TGFbeta-induced phosphorylation of Par6 promotes migration and invasion in prostate cancer cells. Br J Cancer 112: 1223-31

Mungamuri SK, Murk W, Grumolato L, Bernstein E, Aaronson SA (2013) Chromatin modifications sequentially enhance ErbB2 expression in ErbB2-positive breast cancers. Cell Rep 5: 302-13

Nieto MA (2013) Epithelial plasticity: a common theme in embryonic and cancer cells. Science 342: 1234850

Nishida J, Miyazono K, Ehata S (2018) Decreased TGFBR3/betaglycan expression enhances the metastatic abilities of renal cell carcinoma cells through TGF-beta-dependent and -independent mechanisms. Oncogene 37: 2197-2212

Papageorgis P, Lambert AW, Ozturk S, Gao F, Pan H, Manne U, Alekseyev YO, Thiagalingam A, Abdolmaleky HM, Lenburg M, Thiagalingam S (2010) Smad signaling is required to maintain epigenetic silencing during breast cancer progression. Cancer Res 70: 968-78

Pedersen MH, Hood BL, Beck HC, Conrads TP, Ditzel HJ, Leth-Larsen R (2017) Downregulation of antigen presentation-associated pathway proteins is linked to poor outcome in triple-negative breast cancer patient tumors. Oncoimmunology 6: e1305531

bioRxiv preprint doi: https://doi.org/10.1101/348532; this version posted June 16, 2018. The copyright holder for this preprint (which was not certified by peer review) is the author/funder. All rights reserved. No reuse allowed without permission.

Peinado H, Ballestar E, Esteller M, Cano A (2004) Snail mediates E-cadherin repression by the recruitment of the Sin3A/histone deacetylase 1 (HDAC1)/HDAC2 complex. Mol Cell Biol 24: 306-19

Polyak K (2011) Heterogeneity in breast cancer. J Clin Invest 121: 3786-8

Prat A, Karginova O, Parker JS, Fan C, He X, Bixby L, Harrell JC, Roman E, Adamo B, Troester M, Perou CM (2013) Characterization of cell lines derived from breast cancers and normal mammary tissues for the study of the intrinsic molecular subtypes. Breast Cancer Res Treat 142: 237-55

Rovini A, Gauthier G, Berges R, Kruczynski A, Braguer D, Honore S (2013) Anti-migratory effect of vinflunine in endothelial and glioblastoma cells is associated with changes in EB1 C-terminal detyrosinated/tyrosinated status. PLoS One 8: e65694

Singh R, Yadav V, Kumar S, Saini N (2015) MicroRNA-195 inhibits proliferation, invasion and metastasis in breast cancer cells by targeting FASN, HMGCR, ACACA and CYP27B1. Sci Rep 5: 17454

Skrypek N, Goossens S, De Smedt E, Vandamme N, Berx G (2017) Epithelial-to-Mesenchymal Transition: Epigenetic Reprogramming Driving Cellular Plasticity. Trends Genet 33: 943-959

Smollich M, Gotte M, Yip GW, Yong ES, Kersting C, Fischgrabe J, Radke I, Kiesel L, Wulfing P (2007) On the role of endothelin-converting enzyme-1 (ECE-1) and neprilysin in human breast cancer. Breast Cancer Res Treat 106: 361-9

bioRxiv preprint doi: https://doi.org/10.1101/348532; this version posted June 16, 2018. The copyright holder for this preprint (which was not certified by peer review) is the author/funder. All rights reserved. No reuse allowed without permission.

Tan X, Chen S, Wu J, Lin J, Pan C, Ying X, Pan Z, Qiu L, Liu R, Geng R, Huang W (2017) PI3K/AKT-mediated upregulation of WDR5 promotes colorectal cancer metastasis by directly targeting ZNF407. Cell Death Dis 8: e2686

Tang B, Vu M, Booker T, Santner SJ, Miller FR, Anver MR, Wakefield LM (2003) TGF-beta switches from tumor suppressor to prometastatic factor in a model of breast cancer progression. J Clin Invest 112: 1116-24

Thiery JP, Sleeman JP (2006) Complex networks orchestrate epithelial-mesenchymal transitions. Nat Rev Mol Cell Biol 7: 131-42

Viloria-Petit AM, David L, Jia JY, Erdemir T, Bane AL, Pinnaduwage D, Roncari L, Narimatsu M, Bose R, Moffat J, Wong JW, Kerbel RS, O'Malley FP, Andrulis IL, Wrana JL (2009) A role for the TGFbeta-Par6 polarity pathway in breast cancer progression. Proc Natl Acad Sci U S A 106: 14028-33

Wan F, Peng L, Zhu C, Zhang X, Chen F, Liu T (2017) Knockdown of Latent Transforming Growth Factor-beta (TGF-beta)-Binding Protein 2 (LTBP2) Inhibits Invasion and Tumorigenesis in Thyroid Carcinoma Cells. Oncol Res 25: 503-510

Wang F, Han J, Wang L, Jing Y, Zhu Z, Hui D, Wang Z, Wang Y, Dong Y, Tan T (2017) CCCTC-Binding Factor Transcriptionally Targets Wdr5 to Mediate Somatic Cell Reprogramming. Stem Cells Dev 26: 743-750

bioRxiv preprint doi: https://doi.org/10.1101/348532; this version posted June 16, 2018. The copyright holder for this preprint (which was not certified by peer review) is the author/funder. All rights reserved. No reuse allowed without permission.

Wu MZ, Tsai YP, Yang MH, Huang CH, Chang SY, Chang CC, Teng SC, Wu KJ (2011) Interplay between HDAC3 and WDR5 is essential for hypoxia-induced epithelial-mesenchymal transition. Mol Cell 43: 811-22

Wu Q, Xiang S, Ma J, Hui P, Wang T, Meng W, Shi M, Wang Y (2018a) Long non-coding RNA CASC15 regulates gastric cancer cell proliferation, migration and epithelial mesenchymal transition by targeting CDKN1A and ZEB1. Molecular oncology

Wu Y, Diao P, Li Z, Zhang W, Wang D, Wang Y, Cheng J (2018b) Overexpression of WD repeat domain 5 associates with aggressive clinicopathological features and unfavorable prognosis in head neck squamous cell carcinoma. J Oral Pathol Med

Yu M, Bardia A, Wittner BS, Stott SL, Smas ME, Ting DT, Isakoff SJ, Ciciliano JC, Wells MN, Shah AM, Concannon KF, Donaldson MC, Sequist LV, Brachtel E, Sgroi D, Baselga J, Ramaswamy S, Toner M, Haber DA, Maheswaran S (2013) Circulating breast tumor cells exhibit dynamic changes in epithelial and mesenchymal composition. Science 339: 580-4

Zhang H, Meng F, Wu S, Kreike B, Sethi S, Chen W, Miller FR, Wu G (2011) Engagement of I-branching {beta}-1, 6-N-acetylglucosaminyltransferase 2 in breast cancer metastasis and TGF-{beta} signaling. Cancer Res 71: 4846-56

bioRxiv preprint doi: https://doi.org/10.1101/348532; this version posted June 16, 2018. The copyright holder for this preprint (which was not certified by peer review) is the author/funder. All rights reserved. No reuse allowed without permission.

Figures legend

Figure 1. WDR5 is overexpressed in breast cancer and controls tumorigenesis. (A-B) MCF10DCIS cell line was infected to silence WDR5 (shWDR5) or a neutral control (shLuc) and inoculated *in vivo* in immunocompromised mice (n=5 per group) or plated for *in vitro* proliferation assays (n=3). A) Dot plots represent tumor volume in shWDR5 or shLuc MCF10DCIS (mean ± SD - cm^3). Statistical significance was determined using an unpaired Student *t* test (***: P<0.001). B) *In vitro* relative proliferation values of shWDR5 in MCF10DCIS cells are reported with respect to control shLuc. Statistical significance was determined using an unpaired Student *t* test (***: P<0.001). (C-D) A small molecule inhibitor of *WDR5*, OICR-9429, was used at increasing concentration in MCF10DCIS cells. C) Images and corresponding histograms represented cell clonogenicity expressed as mean ± SD of a biological triplicate after 6 days of treatment. Cells were stained with crystal violet and quantified by using ImageJ analysis. D) Effect of OICR-9429 on MCF10DCIS viability was evaluated after 3 days of treatment and expressed as mean ± SD of a biological triplicate. Statistical significance was determined using an unpaired Student *t* test (*: P<0.05; **:P<0.01; ***: P<0.001). E) WDR5 expression was detected in normal breast tissues (n=11) and Metastatic Breast Cancer (MBC) PDXs (n=8) by IHC. Representative samples of normal and MBC PDX were shown. Scale bar 100μm. Box plots represent WDR5 expression quantified by using Fiji tools for DAB positivity. Statistical significance was determined using an unpaired Student *t* test (***: P<0.001). F) Six MBC PDXs were infected to target control (shLuc) and shWDR5. Transduced cells were transplanted in NSG mice. Dot plots represent tumor volume (mean ± SD – cm^3) of three to four tumors *per*

bioRxiv preprint doi: https://doi.org/10.1101/348532; this version posted June 16, 2018. The copyright holder for this preprint (which was not certified by peer review) is the author/funder. All rights reserved. No reuse allowed without permission.

group. Statistical significances were calculated by applying an unpaired Student *t* test (**: P<0.01; ***: P<0.001).

Figure 2. WDR5 silencing significantly affected breast cancer metastasization. Effect of WDR5 silencing was studied in MDA-MB-231 as breast cancer metastatic model. A) MDA-MB-231 cells were infected to express Luciferase, transduced to silence WDR5 or a control vector (SCR) and then transplanted in NSG mice (n=5 per group). Metastasis detection at distant organs was performed by using bioluminescence technique *in vivo* after resection of primary tumors. B) Relative migration was performed on transwells (n=3), stained by crystal violet and represented as ratio of shWDR5 and shLuc values. Statistical significance was determined using an unpaired Student *t* test (***: P<0.001). C) Cells from MBC PDXs were used for *in vitro* migration study in duplicate. Relative migration (mean ± SD) was calculated by ImageJ analysis on Crystal violet staining positivity and expressed as ratio of silenced versus control values. Statistical significances were calculated by applying an unpaired Student *t* test (*: P<0.05; **: P<0.01). D) Metastasis free survival in breast cancer patients (n=295) was calculated in WDR5-low and WDR5-high groups divided at median of gene expression. Statistic comparison was performed using log rank test. E) WDR5 expression was considered with respect to estrogen status, or chemotherapy or endocrine therapy and Hazard Ratio (HR), confidence interval (CI)(95%) and P value were calculated.

Figure 3. WDR5 silencing inhibits EMT in breast cancer.

RNA-seq was performed in 5 PDXs upon WDR5 silencing. A) Pie charts showed differentially expressed genes (DEGs) obtained by pairwise analysis in each PDX comparing shLuc and shWDR5 MBC PDXs cells. Genes were identified as DEGs when

bioRxiv preprint doi: https://doi.org/10.1101/348532; this version posted June 16, 2018. The copyright holder for this preprint (which was not certified by peer review) is the author/funder. All rights reserved. No reuse allowed without permission.

the following criteria were met: $\log_2$ fold-change (FC) ≥ |0.6|, false discovery rate (FDR) < 0.05 and expression > 0.5 RPKM. DEGs in common at least in two PDXs defined a Golden Genes Set (GGS). B) Heatmap showed normalized expression values after removing batch effects using 253 DEGs belonging to GGS. Blue and orange colors indicate down- and up-regulated genes, respectively. C) Representative Gene Ontology terms enriched in DEGs are shown. For complete list refer to Appendix Table S2. D) Morphological changes by actin cytoskeleton remodeling in MCF10DCIS breast cancer cell line due to *WDR5* silencing were evaluated by immunofluorescence technique (n=3). Images show F-actin, DAPI and merged staining in shLuc and shWDR5 cells. E) Adhesion to a panel of substrates (collagen - CL, laminin - LM, fibronectin - FN, matrigel - MG) in shLuc or shWDR5 cells was considered (n=3). Cells were stained by crystal violet and adhesion percentage was calculated by ImageJ and expressed as ratio of relative cells area of shWDR5 versus shLuc. Statistical significances among areas were calculated by applying an unpaired Student *t*-test (***: P<0.001). F) Effect of WDR5 silencing on E-cadherin (CDH1) and Vimentin (VIM) expression was detected by western blot in PDXs used for transcriptomic analysis. Vinculin was used as normalizer.

Figure 4. WDR5 regulates its targets by histone methylation.

A) Box plots show H3K4me3 signal intensity in shLuc and shWDR5 MCF10DCIS cancer cell lines at gene promoters. Central values represent the median, the bars the 25th and 75th percentile and the dashed lines the lower and upper whiskers. P-value was obtained from a Wilcoxon rank-sum test. B) Snapshot represents WDR5 and H3K4me3 binding peaks identified by ChIP-seq analysis and RNA signal of TGFβ1 gene in a representative replicate of shLuc and shWDR5 MCF10DCIS cells. C) Box plots show Log2FC values for each gene belonging to TGFβ pathway highlighted by Gene Ontology analysis in 5 MBC

bioRxiv preprint doi: https://doi.org/10.1101/348532; this version posted June 16, 2018. The copyright holder for this preprint (which was not certified by peer review) is the author/funder. All rights reserved. No reuse allowed without permission.

PDXs. D) Representative IPA upstream pathways enriched in Golden Genes Set of PDXs are shown. For complete list refer to Appendix Table S2. E) Volcano plot shows Differentially Expressed Genes (DEGs) in shWDR5 MCF10DCIS cancer cell line. The log2 expression fold change (FC) is shown on the horizontal axis and -log10 of the FDR is shown on the vertical axis. Up-regulated genes (FDR < 0.05 and log2 FC > 0.6) are highlighted in orange while down-regulated genes in blue (FDR < 0.05 and log2 FC < -0.6). The genes indicated in green are also down-regulated in the PDX set. F) Dot plots represent Log2FC values for each gene in MBC PDXs. Dashed line represents threshold imposed on Log2FC to determine DEGs.

Figure 5. EMT and metastasis are regulated by TGFβ1-WDR5 axis in breast cancer. A) Relative expression of CDH2 and TWIST1, SNAI1, SNAI2 and ZEB1 transcription factors in MCF10DCIS breast cancer cell line was analyzed by RT-qPCR. Cells were treated with (+) or without (-) 5 ng/mL of TGFβ1 for 2 days and with (+) or without (-) shWDR5. Statistical significance was determined using an unpaired Student *t* test (*: P<0.05; **: P<0.01; ***: P<0.001) B) Migration of MCF10DCIS cells treated with (+) or without (-) TGFβ1 and with (+) or without (-) shWDR5 is shown. C) Immunoblots for total- (T) or phosphorylated- (P) SMAD2 and SMAD3, and (D) T-ERK and P-ERK were performed in MCF10DCIS cells treated with (+) or without (-) TGFβ1 and with (+) or without (-) shWDR5. GADPH or Vinculin were used as normalizers.

Figure 6. Molecular mechanism of WDR5-TGFβ1 axis in the regulation of EMT in breast cancer cells. A) In breast cancer, silencing of WDR5 is able to induce cell differentiation from an intermediate mesenchymal toward an epithelial–like phenotype

bioRxiv preprint doi: https://doi.org/10.1101/348532; this version posted June 16, 2018. The copyright holder for this preprint (which was not certified by peer review) is the author/funder. All rights reserved. No reuse allowed without permission.

through transcriptional down-regulation of the endogenous levels of TGFβ1 and the contextual down-regulation of H3K4me3 intensity at its promoter. The epithelial trait is supported by the up-regulation of keratins, tight junction (TJ), adherent junction (AJ), remodeling of cytoskeleton and down-regulation of mesenchymal genes. Interestingly, WDR5-dependent reprogramming switches cells from metastable to low metastatic. B) Exogenous TGFβ1 perturbation, frequently observed during metastasization, is able to induce EMT and the metastatic phenotype, by phosphorylation of TGFβ-canonical (SMAD2/3) and non-canonical (ERK1/2) complexes (upper panel). On the contrary, WDR5 silencing partially abrogates phosphorylation, inhibits EMT genes transcription and reduces cell migration, thus bringing breast cancer cells to the previous metastable state (lower panel).

Expanded view Figure Legend

Figure EV 1. WDR5 regulates TGFβ targets. A) Heatmap of Transcription Start Sites (TSS)-proximal WDR5 binding events in the shLuc MCF10DCIS cancer cell line is shown. A 3kb genomic interval centered on the summit of WDR5 peaks is considered. For comparison, the same regions are also shown in shWDR5 MCF10DCIS cells. B) Heatmap represents down- (orange) and up- (blue) regulated genes involved in epithelial and mesenchymal control in MCF10DCIS cell line due to WDR5 silencing. C) DEGs within differentially methylated promoters are shown. Genes with differential expression and differential H3K4me3 but not bound by WDR5 are in gray and genes with differential expression, differential H3K4me3 and bound WDR5 peaks are in red. D) Relative expression of main WDR5 targets highlighted by RNA-seq analysis was detected in

bioRxiv preprint doi: https://doi.org/10.1101/348532; this version posted June 16, 2018. The copyright holder for this preprint (which was not certified by peer review) is the author/funder. All rights reserved. No reuse allowed without permission.

shWDR5 MCF10DCIS cells by RT-qPCR with respect to shLuc. The results are presented as means ± SD of three independent experiments.

Expanded view Table Legend

Table EV 1. WDR5 genome wide binding sites on MCF10DCIS were assigned to the nearest proximal and distal transcription start sites (TSS)(+3kb). H3K4me3 ChIP-seq was performed on MCF10DCIS breast cancer cell line. Reads were mapped to the promoter region (±1'500 bp relative to TSS) for annotated transcripts of DEGs. Significant differential H3K4me3 values are shown.

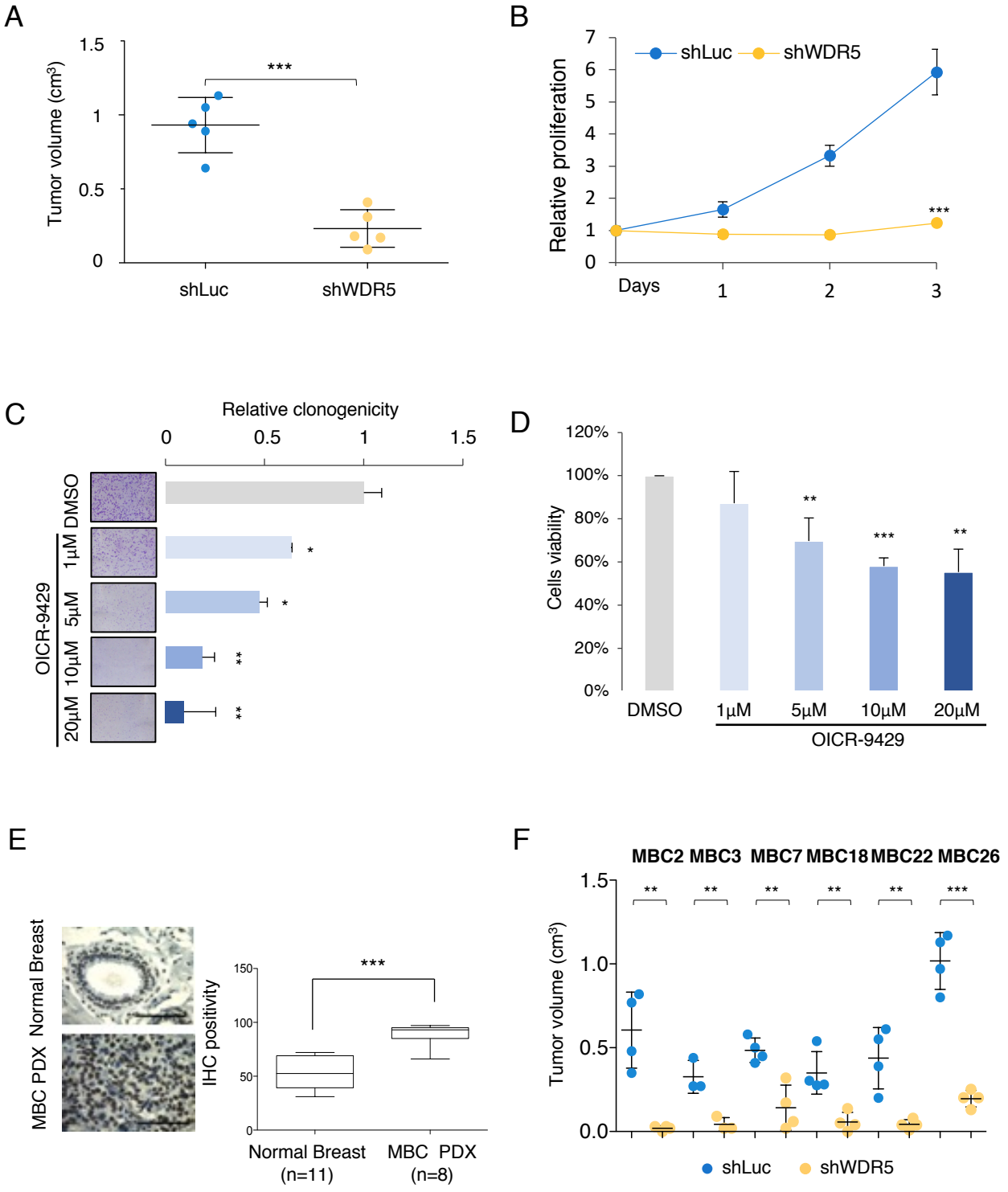
A
Tumor volume (cm3)
1.5
1
0.5
0
***
shLuc
shWDR5
B
Relative proliferation
7
6
5
4
3
2
1
0
shLuc
shWDR5
***
Days
1
2
3
C
Relative clonogenicity
0
0.5
1
1.5
OICR-9429
DMSO
1μM
5μM
10μM
20μM
*
*
**
**
D
Cells viability
120%
100%
80%
60%
40%
20%
0%
**
***
**
DMSO
1μM
5μM
10μM
20μM
OICR-9429
E
MBC PDX
Normal Breast
IHC positivity
150
100
50
0
***
Normal Breast
(n=11)
MBC PDX
(n=8)
F
MBC2 MBC3 MBC7 MBC18 MBC22 MBC26
Tumor volume (cm3)
1.5
1.0
0.5
0.0
**
**
**
**
**
***
shLuc
shWDR5

Figure 1

A

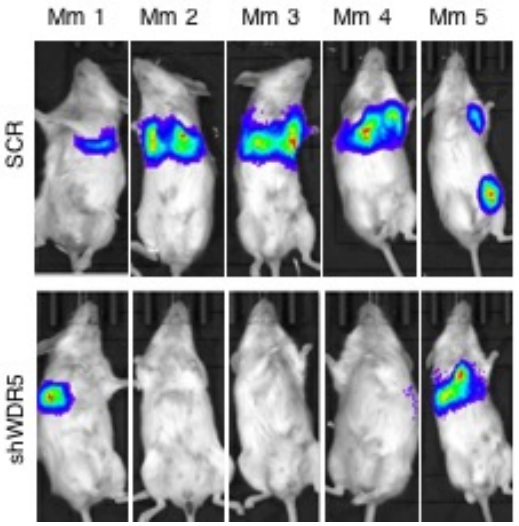

B

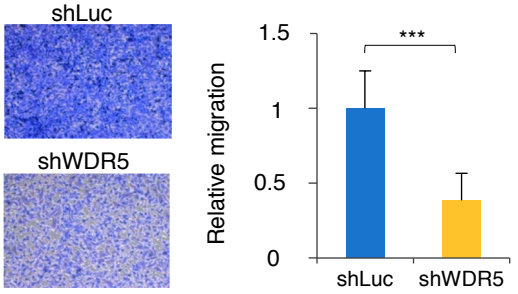

C

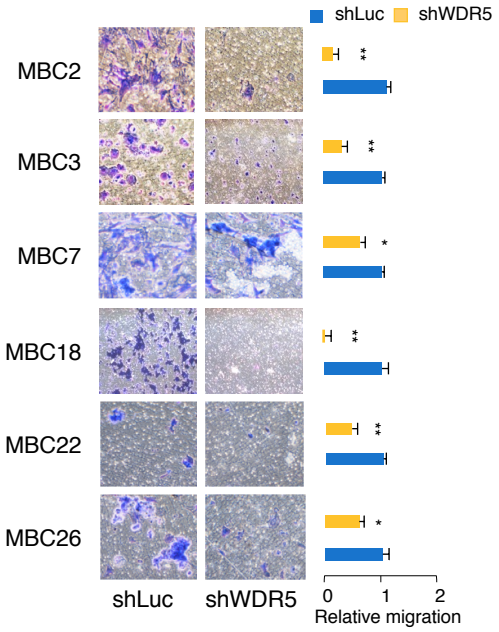

D

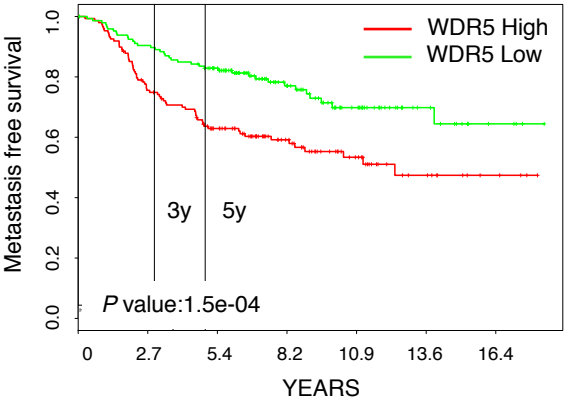

E

Subgroup	HR	CI (95%)	P
Main	1.35	1.16-1.58	1.50E-04
ER status	1.29	1.09-1.53	3.90E-03
Chemotherapy	1.36	1.16-1.58	1.00E-04
Endocrine therapy	1.34	1-15-1.57	2.00E-04

Figure 2

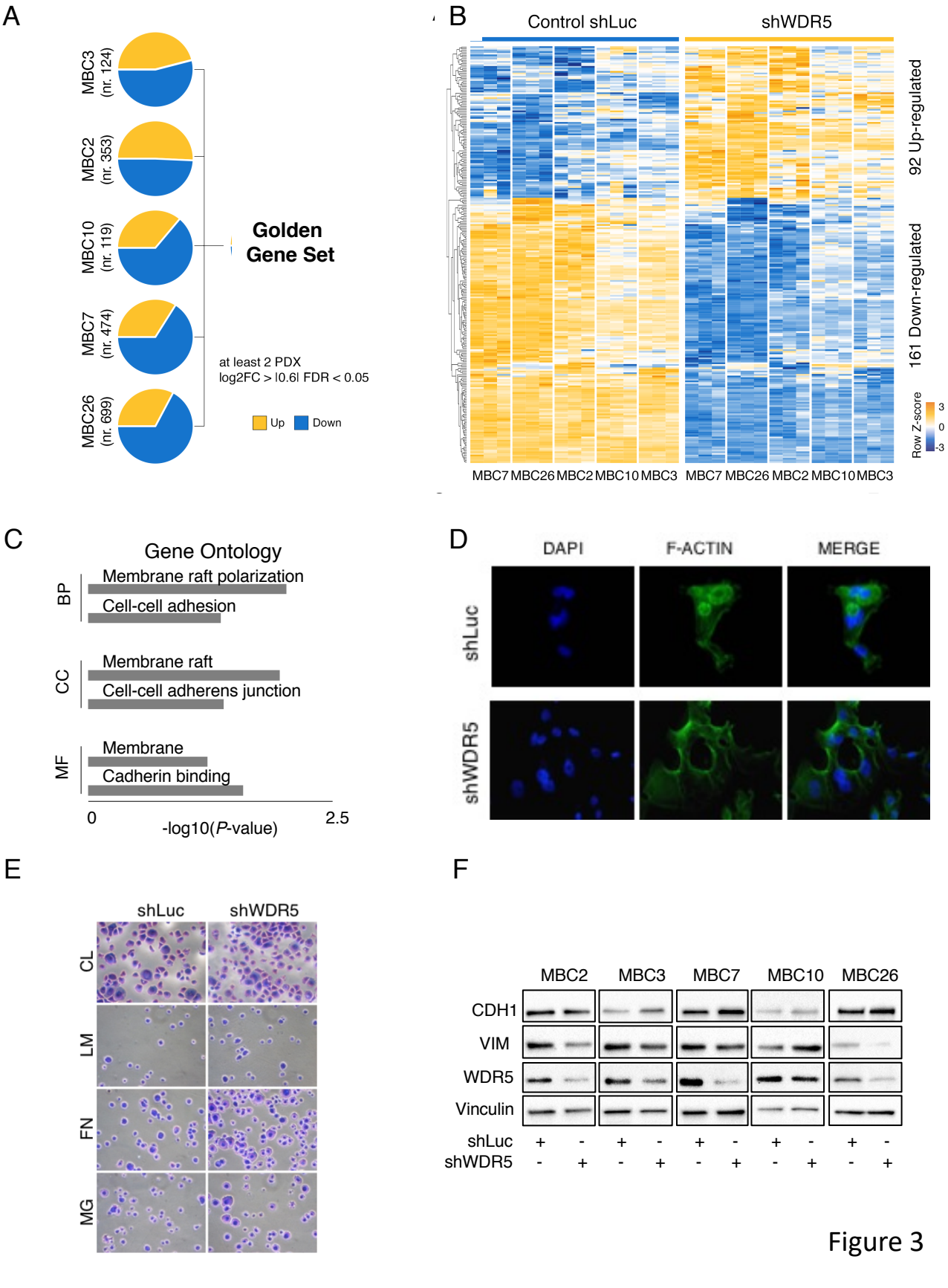
A
MBC3 (nr. 124)
MBC2 (nr. 353)
MBC10 (nr. 119)
MBC7 (nr. 474)
MBC26 (nr. 699)
Golden Gene Set
at least 2 PDX
log2FC > |0.6| FDR < 0.05
Up
Down
B
Control shLuc
shWDR5
92 Up-regulated
161 Down-regulated
Row Z-score
3
0
-3
MBC7 MBC26 MBC2 MBC10 MBC3 MBC7 MBC26 MBC2 MBC10 MBC3
C
Gene Ontology
BP
Membrane raft polarization
Cell-cell adhesion
CC
Membrane raft
Cell-cell adherens junction
MF
Membrane
Cadherin binding
0
2.5
-log10(P-value)
D
DAPI
F-ACTIN
MERGE
shLuc
shWDR5
E
shLuc
shWDR5
CL
LM
FN
MG
F
MBC2
MBC3
MBC7
MBC10
MBC26
CDH1
VIM
WDR5
Vinculin
shLuc + - + - + - + - + -
shWDR5 - + - + - + - + - +

Figure 3

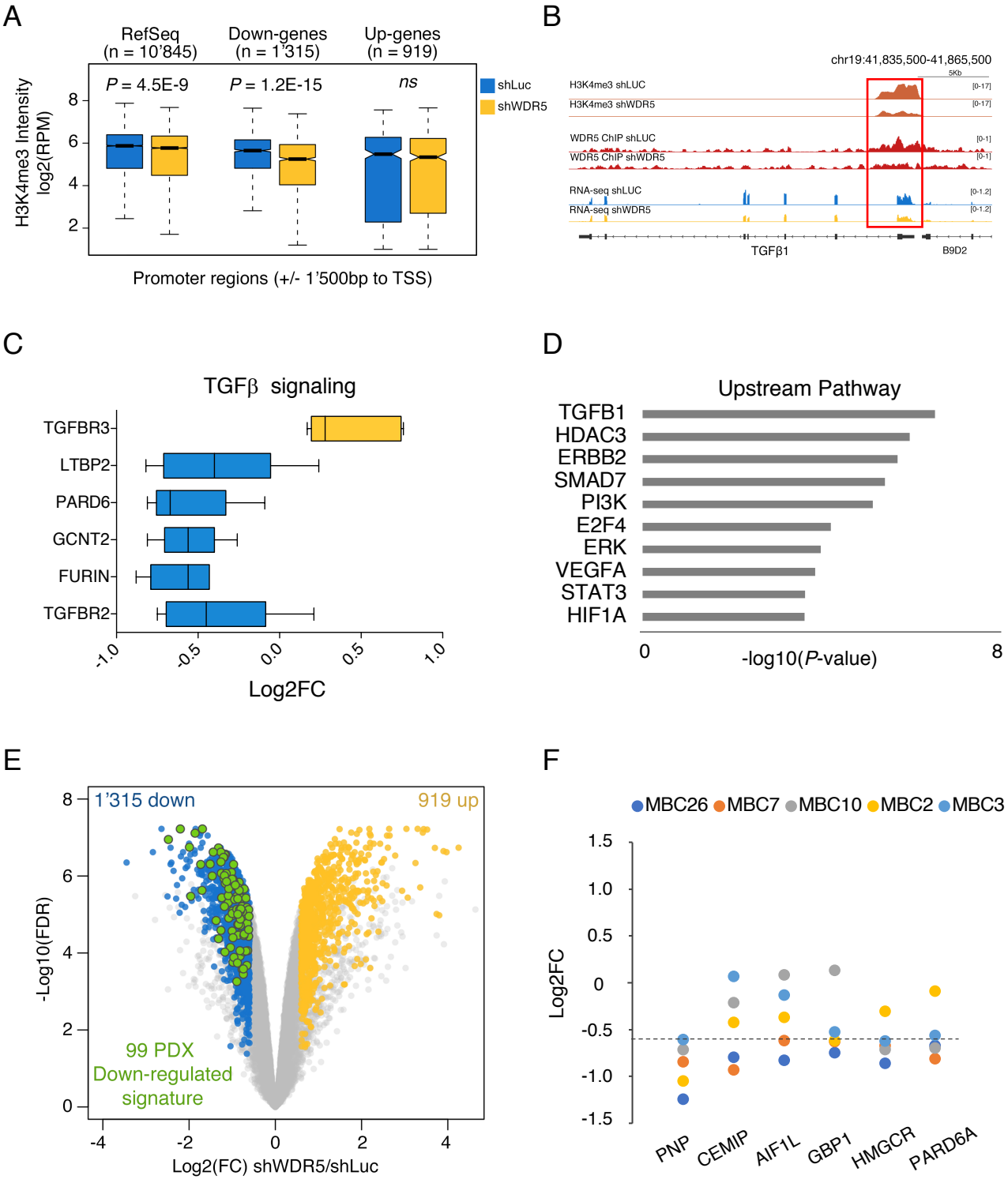
A
RefSeq (n = 10'845)
Down-genes (n = 1'315)
Up-genes (n = 919)
P = 4.5E-9
P = 1.2E-15
ns
shLuc
shWDR5
H3K4me3 Intensity log2(RPM)
Promoter regions (+/- 1'500bp to TSS)
B
chr19:41,835,500-41,865,500
H3K4me3 shLUC
H3K4me3 shWDR5
WDR5 ChIP shLUC
WDR5 ChIP shWDR5
RNA-seq shLUC
RNA-seq shWDR5
TGFβ1
B9D2
C
TGFβ signaling
TGFBR3
LTBP2
PARD6
GCNT2
FURIN
TGFBR2
Log2FC
D
Upstream Pathway
TGFB1
HDAC3
ERBB2
SMAD7
PI3K
E2F4
ERK
VEGFA
STAT3
HIF1A
-log10(P-value)
E
1'315 down
919 up
99 PDX Down-regulated signature
-Log10(FDR)
Log2(FC) shWDR5/shLuc
F
MBC26
MBC7
MBC10
MBC2
MBC3
Log2FC
PNP
CEMIP
AIF1L
GBP1
HMGCR
PARD6A

Figure 4

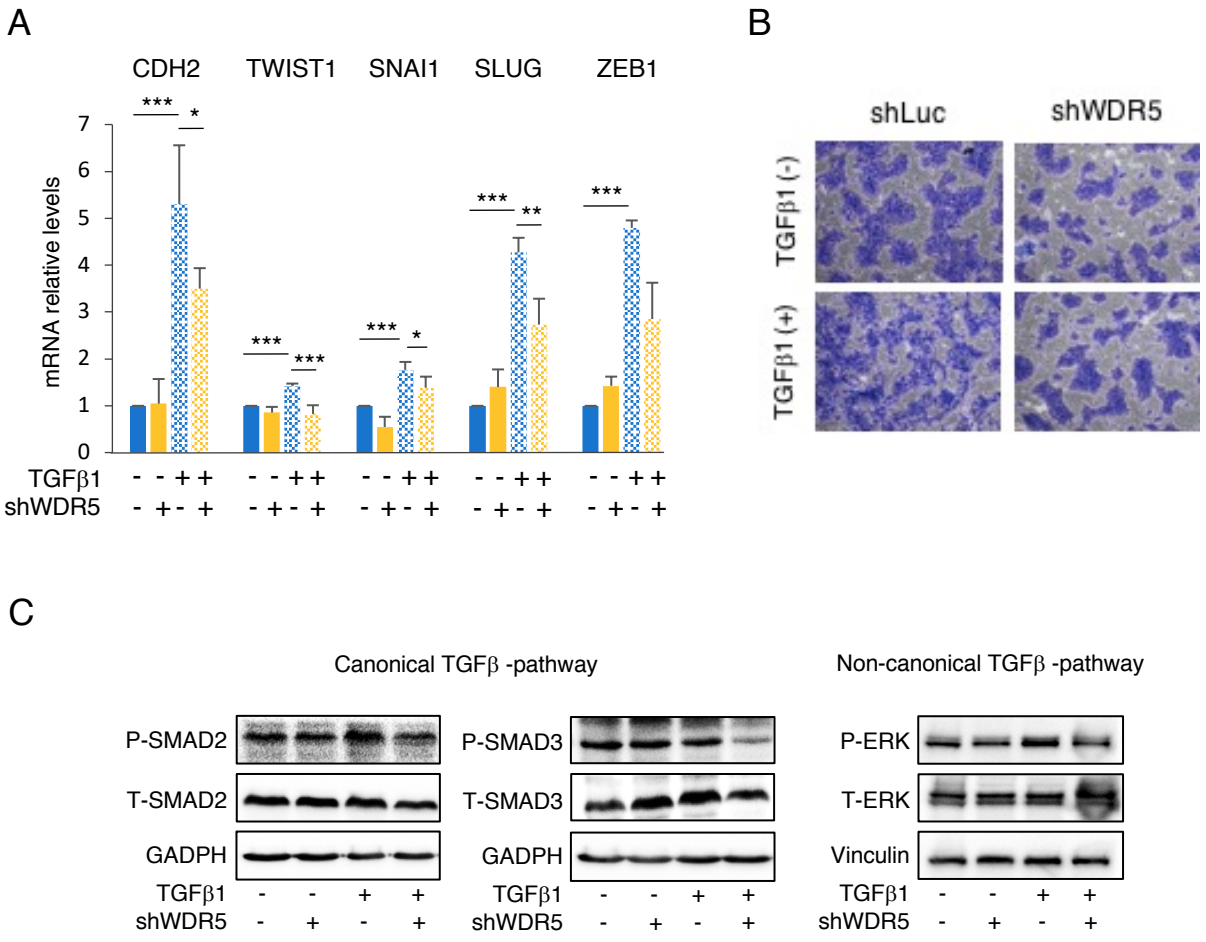
A
CDH2
TWIST1
SNAI1
SLUG
ZEB1
mRNA relative levels
TGFβ1
shWDR5
B
shLuc
shWDR5
TGFβ1 (-)
TGFβ1 (+)
C
Canonical TGFβ -pathway
Non-canonical TGFβ -pathway
P-SMAD2
T-SMAD2
GADPH
P-SMAD3
T-SMAD3
GADPH
P-ERK
T-ERK
Vinculin
TGFβ1
shWDR5

Figure 5

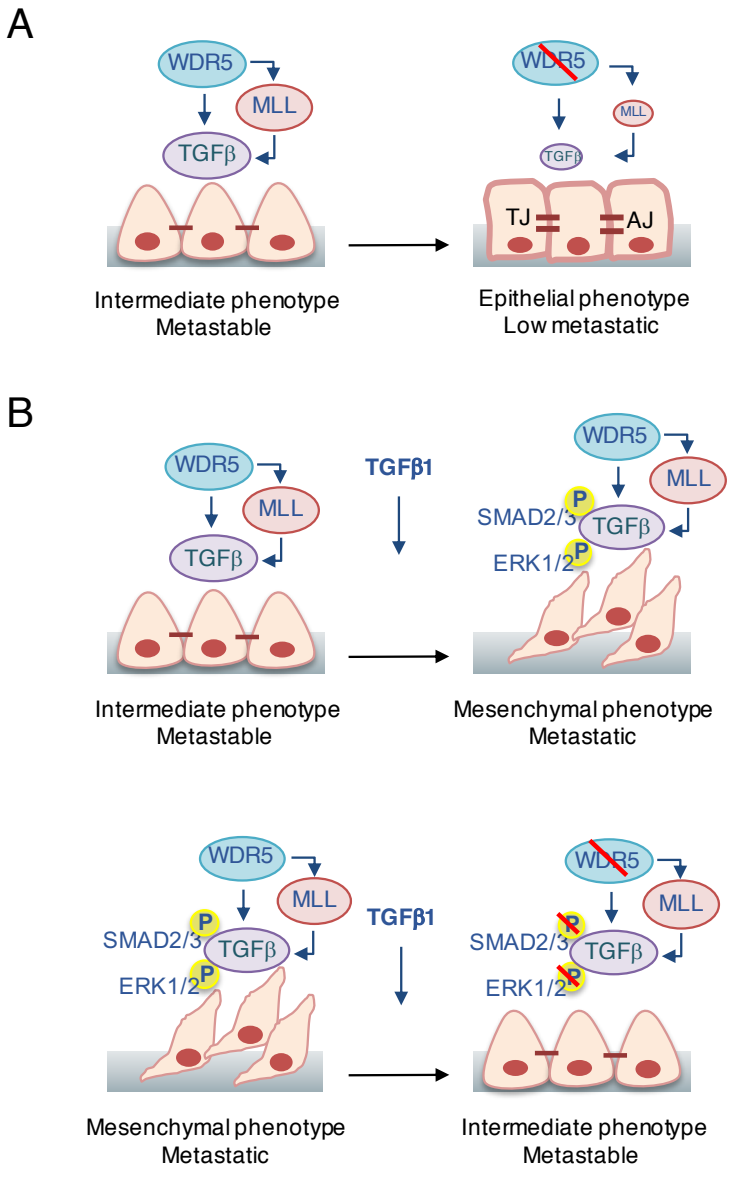
A
WDR5
MLL
TGFβ
TJ
AJ
Intermediate phenotype
Metastable
Epithelial phenotype
Low metastatic
B
TGFβ1
SMAD2/3
ERK1/2
P
Intermediate phenotype
Metastable
Mesenchymal phenotype
Metastatic
Mesenchymal phenotype
Metastatic
Intermediate phenotype
Metastable

Figure 6

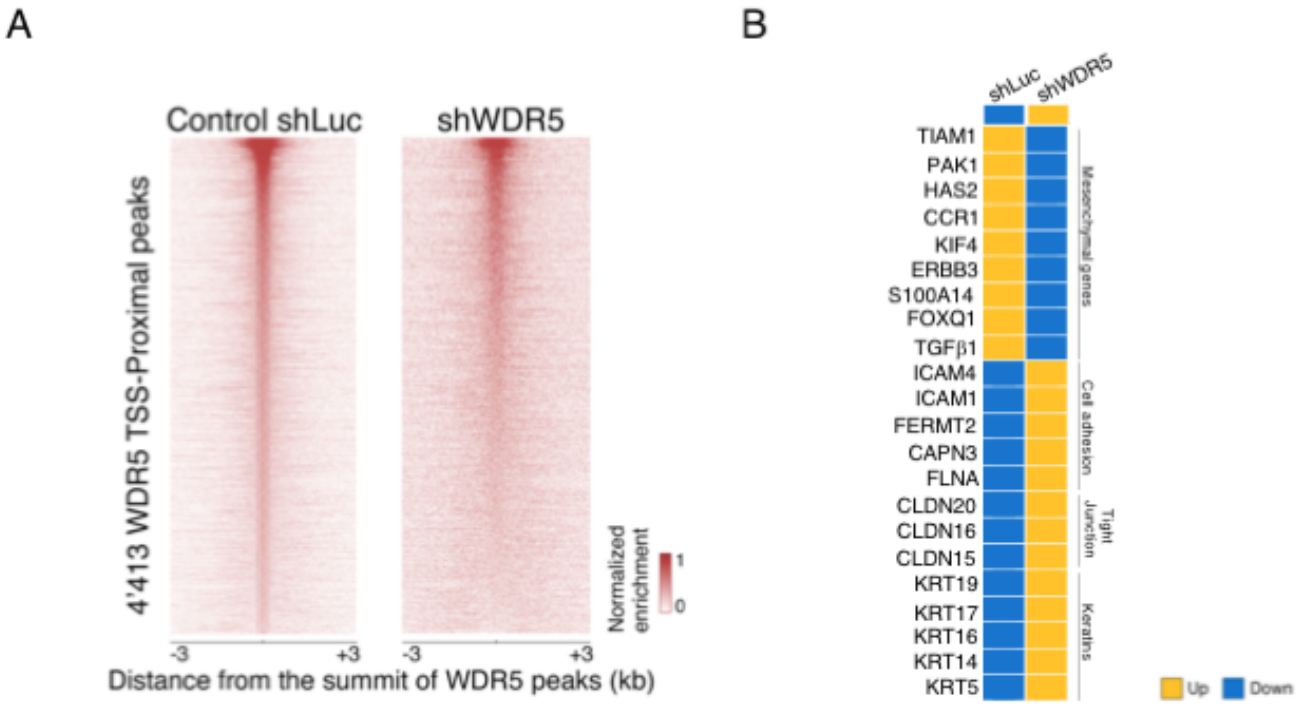

Expanded view Figure EV1